

High-Field Superconducting Halo in UTe_2

Sylvia K. Lewin^{1,2,*}, Peter Czajka^{1,2,*}, Corey E. Frank^{1,2}, Gicela Saucedo Salas², Hyeok Yoon², Yun Suk Eo², Johnpierre Paglione^{2,3}, Andriy H. Nevidomskyy⁴, John Singleton⁵, and Nicholas P. Butch^{1,2}

¹*NIST Center for Neutron Research, National Institute of Standards and Technology, Gaithersburg, MD, USA*

²*Maryland Quantum Materials Center, Department of Physics, University of Maryland, College Park, MD, USA*

³*Canadian Institute for Advanced Research, Toronto, Ontario M5G 1Z8, Canada*

⁴*Department of Physics and Astronomy, Rice University, Houston, TX, USA and*

⁵*National High Magnetic Field Laboratory, Los Alamos National Laboratory, Los Alamos, NM, USA*

(Dated: February 29, 2024)

Heavy fermion UTe_2 is a promising candidate for topological superconductivity that also exhibits multiple high-field superconducting phases. The SC_{FP} phase has only been observed in off-axis magnetic fields in the bc plane at fields greater than 40 teslas, a striking scale given its critical temperature of only 2 kelvins. Here, we extend measurements of this unique superconducting state outside of the bc plane and reveal its core structure. The SC_{FP} phase is not confined to fields in the bc plane and in fact wraps around the b axis in a halo-like fashion. In other words, this superconducting state, which exists in fields above 73 teslas, is stabilized by a field component perpendicular to the magnetic easy axis. These remarkable field scales further underscore UTe_2 's unique magnetophilic superconducting tendencies and suggest an underlying pairing mechanism that is qualitatively distinct from known theories for field-enhanced superconductivity. Phenomenological modeling points to a two-component, non-unitary spin triplet order parameter with finite orbital momentum of the Cooper pairs as a natural explanation for the field-angle dependence of the upper critical field of the SC_{FP} phase.

Magnetic fields typically act to destroy superconductivity, a fact that places strict physical limitations on superconducting technologies. Heavy fermion material UTe_2 represents a striking exception to this conventional phenomenology [1–4]. In addition to harboring a low-field superconducting state that is of interest for topological quantum computing applications [5, 6], the material also exhibits additional superconducting phases that only exist at extraordinarily high magnetic fields, as illustrated in the full phase diagram in Fig. 1a. These include a field-reinforced state that exists up to 34 T for \mathbf{H} aligned close to the UTe_2 b axis (SC_2) [2, 7] as well as an even more exotic phase that has only been observed by tilting \mathbf{H} approximately $20\text{--}40^\circ$ from b towards c (SC_{FP}) [2]. The latter, which is the focus of the present study, only exists within the field-polarized (FP) state that is separated from the low-field regime by a metamagnetic transition (pink sheet in Fig. 1a). Remarkably, the SC_{FP} phase only onsets above 40 T and persists up to at least 73 T. These field scales are particularly impressive given UTe_2 's relatively low T_c (1.6–2.1 K depending on sample) [1, 8]. We also emphasize that the material is fairly three-dimensional [9, 10], which requires the superconductivity to be robust against orbital as well as spin-based depairing mechanisms, unlike the numerous Pauli limit-breaking 2D systems for which high critical fields are only seen when \mathbf{H} is directed within the conducting plane [11–13]. It also differs from other uranium-based superconductors for which field-enhanced pairing is more

straightforwardly associated with specific phase boundaries and high-symmetry directions [14, 15].

Prior experiments on the SC_{FP} phase have been limited to crystallographic planes. Superconductivity was found with magnetic fields applied in the bc plane [2, 16], but not the ab plane [2], which has fueled speculation that there may be some special angle within the bc plane that permits this unique high-field phase [16]. In this study, we map the SC_{FP} phase boundaries outside the bc plane and find that SC_{FP} actually wraps around b in a halo-like fashion (high H blue region in Fig. 1a). We emphasize that Fig. 1a is an illustration intended to capture broad features in an extended data set.

All measurements were performed at the National High Magnetic Field Laboratory's Pulsed Field Facility at Los Alamos National Laboratory. Data were primarily taken in a 65 T magnet system (typical field pulses were 60 T) as well as a 75 T duplex magnet (typical field pulses were 73 T). Lacking a dual axis rotator suitable for pulsed fields, we utilized a single axis rotator with the crystal manually placed on the sample platform such that \mathbf{H} is applied at some angle θ_{bc} within the bc plane (see Fig. 1b). The rotator is then used to apply field pulses at various tilt angles θ_a towards the UTe_2 a axis. An example of this for $\theta_{bc} = 40^\circ$ is shown in Fig. 1c. A high-field zero resistance state is obtained when \mathbf{H} is applied within the bc plane ($\theta_a \approx 0^\circ$). As \mathbf{H} is tilted towards a , the H window in which superconductivity is observed shrinks until it is lost entirely around $\theta_a = 12.6^\circ$. For $\theta_a \geq 12.6^\circ$ the resistance instead shows a sharp increase, which is a signature of the metamagnetic transition [17].

For some samples we utilized a contactless conductivity technique: Proximity Detector Oscillator (PDO) mea-

* These authors contributed equally: Sylvia K. Lewin and Peter Czajka

measurements [18]. UTe_2 's low electrical resistivity and challenging surface chemistry can make traditional electrical resistivity measurements difficult, especially in pulsed field. PDO experiments circumvent these technical obstacles and are a well established technique for determining phase boundaries in UTe_2 and other superconductors [2, 19–24]. This is illustrated in Fig. 1d. At 0.64 K, dramatic shifts in PDO frequency f are seen at 8 and 45 T. Higher f is associated with lower resistance; the regions of elevated f are superconducting. As T is increased, the superconducting phase boundaries shift in the expected fashion and at 2.09 K they are no longer observed. We instead observe a kink downwards at 45 T, indicating a transition to a high-resistance FP phase. An extended discussion of PDO data analysis is provided in the Supplementary Materials.

Fig. 2 displays a set of field pulses and corresponding phase diagrams measured at three different θ_{bc} . The core finding of this experiment is immediately apparent. As θ_{bc} decreases (the measurement plane moves closer to the ab plane) the effect of tilting towards a changes dramatically. For $\theta_{bc} = 30^\circ$ we observe that increasing θ_a initially causes an enhancement of superconductivity instead of the immediate suppression seen in Fig. 1c. As θ_a is increased further, the critical field peaks around 60 T and then decreases until superconductivity is lost entirely around 15.5° , leaving a U-shaped region of superconductivity. The lower boundary tracks the angular evolution of H_m since SC_{FP} only exists within the FP phase and not in the low H state.

At $\theta_{bc} = 23^\circ$, no superconductivity is observed in the bc plane ($\theta_a = 0$). However, we find that tilting \mathbf{H} towards a (by 10°) induces superconductivity. Superconductivity persists up to $\theta_a = 16^\circ$, beyond which a metamagnetic transition is again observed. Similar behavior is observed at $\theta_{bc} = 8^\circ$ (nearly in the ab plane) except that the onset θ_a and $H_{\text{SC}}^{\text{on}}$ have been pushed even higher. This reveals a superconducting regime that only appears at 59 T and persists well above 73 T (judging by the behavior of f vs. H near the maximum field). It also appears that the angular window of superconductivity may narrow substantially at low θ_{bc} . However, it is difficult to say with certainty since this may be related to sample heating due to P2's large size. See the Supplementary Materials for more information.

Fig. 3a shows all phase diagrams measured in this experiment. This includes the PDO data presented in Fig. 2 as well as electrical resistance measurements performed on two additional samples. The electrical resistance measurements confirm the key findings from the PDO data. An initial enhancement of $H_{\text{SC}}^{\text{off}}$ for the SC_{FP} phase is observed at $\theta_{bc} = 29^\circ$ and the recovery of superconductivity by a axis tilting is seen at $\theta_{bc} = 18^\circ$. Stitching phase boundaries from these various θ_{bc} measurement planes together reveals the true structure of the SC_{FP} phase (illustrated in Fig. 1a). The region of superconductivity wraps around b with $H_{\text{SC}}^{\text{on}}$ lowest within the bc plane and highest as \mathbf{H} approaches the ab plane, reflecting the rapid

increase of H_m with θ_a . This anisotropy is responsible for the saddle-like appearance in Fig. 1a.

In Fig. 3b, we construct a simpler picture that captures the primary revelation of this experiment. We ignore H and plot the θ_{bc} and θ_a values at which an SC_{FP} phase is observed as closed points and the values where only H_m is seen as open circles. Note that the data have been symmetrized to fill all four quadrants. Blue shading is added as a guide to the eye as there is some inevitable scatter in the angular phase boundaries caused by sample dependence, angle uncertainty, and differing measurement techniques. Also note that while we did not observe superconductivity within the ab plane, it may just be that $H_{\text{SC}}^{\text{on}}$ in that plane exceeds the 73 T maximum field of the experiment. Our efforts are summarized in the Supplementary Materials. Regardless of whether the SC_{FP} truly does extend to the ab plane, the curvature of the phase boundaries is unambiguous. A finite tilt of \mathbf{H} off b is what ultimately produces this unprecedented extreme high-field superconducting state. This contrasts with earlier investigations that pointed to a particular direction within the bc plane being special. The onset angle off b for superconductivity seems to be around 20° (or alternatively a perpendicular field H_\perp of about 17 T) with some weak dependence on direction and sample characteristics.

Despite the apparent similarities between θ_a and θ_{bc} in their relation to superconductivity, the two directions are crystallographically distinct. This anisotropy is apparent in the angular evolution of the FP phase boundaries [2] and understanding of its interplay with the superconducting halo will be key for identifying the pairing mechanism and (likely triplet) order parameter. Within the bc plane, H_m follows $H_m = H_m^b / \cos(\theta_{bc})$ where $H_m^b \approx 34$ T represents a typical value of H_m for $\mathbf{H} \parallel b$ [2, 25]. In other words the metamagnetic transition occurs when $H_b \approx 34$ T, regardless of H_c . For \mathbf{H} directed outside the bc plane, H_m instead shows a much steeper angle dependence that does not respect this field projection pattern:

$$H_m = H_m^0 + \alpha_2 \sin^2 \theta_a + \alpha_4 \sin^4 \theta_a \quad (1)$$

where H_m^0 is the value of H_m in the bc plane. It is clear that the U-shaped H_m envelope (which serves as a lower bound for SC_{FP}) shifts to higher H as θ_{bc} increases. We fit the individual $H_m(\theta_a)$ curves to eq. (1) and obtain two key findings. First, the function describes the data remarkably well. Second, the fitting parameters α_2 and α_4 are independent of θ_{bc} . The only thing that varies is the bc -plane onset field H_m^0 . This point is illustrated in Fig. 3c where we plot $H_m - H_m^0$ vs. θ_a for all fixed θ_{bc} data sets and find that they all collapse on top of each other. Fitting all phase boundaries together yields values: $\alpha_2 = 94.84$ T, $\alpha_4 = 1933.62$ T. This scaling consistency indicates that tilts towards a and c have orthogonal effects on the FP phase, in contrast to their effects on the superconducting phase.

Our measured bounds of the SC_{FP} state indicate that the phase must be robust against orbital depairing effects

as well as spin-based ones. A likely triplet pairing state naturally accounts for the stability against paramagnetic depairing, but would not explain the orbital resilience. In 2D materials, there is no orbital motion from in-plane fields. But it is not possible to have a complete absence of induced orbital motion for all of the field directions at which SC_{FP} occurs.

Because the SC_{FP} phase only arises within the FP state, magnetic fluctuations likely play a role in mediating the superconducting pairing. Notably, b is the likely magnetic easy axis in the FP phase [26]. In this context, the field-angle dependence of the superconducting halo also indicates that magnetism plays an important role. However, the specific interactions are not understood. Superconductivity in other uranium-based superconductors is often attributed to ferromagnetic spin fluctuations [14, 15]. This exact phenomenology cannot be applied to UTe_2 , as UTe_2 is not a ferromagnet and it is not possible to identify the SC_{FP} phase with a second-order phase transition that would naturally provide enhanced spin fluctuations.

Agnostic of the underlying pairing mechanism, we can model the phase diagram of SC_{FP} phenomenologically and calculate the angle dependence of the upper critical field. Our main conclusion is that the observed angle dependence of the upper critical field is most naturally explained if the Cooper pairs carry a finite orbital momentum:

$$\mathbf{m}_{\text{orb}} = \int_{FS} \frac{d^2k}{(2\pi)^2} \left(i\vec{d}_{\mathbf{k}} \times \vec{d}_{\mathbf{k}}^* \right), \quad (2)$$

where $\vec{d}_{\mathbf{k}}$ is the so-called d -vector associated with the spin triplet order parameter. When the resulting orbital momentum, averaged over the Fermi surface, is non-vanishing, it will couple linearly to the magnetic field yielding a term in the free energy of the form $\Delta F = -w\mathbf{B} \cdot \mathbf{m}_{\text{orb}}$ which naturally depends on the field angle, as seen in the experiment.

For the orbital moment to be non-zero requires the order parameter to be multi-component and non-unitary; the latter statement reflecting the fact that the norm of

the order parameter $|\Delta(\mathbf{k})|^2 \propto |\vec{d}_{\mathbf{k}}|^2 \mathbb{1} + \mathbf{m}_{\text{orb}} \cdot \boldsymbol{\sigma}$ is not proportional to the identity matrix. Moreover, for the model to account for the presence of a local maximum of the upper critical fields as a function of θ_a , as well as the previously reported peak in upper critical fields in the bc plane, it is important that \mathbf{m}_{orb} have a dominant c -axis component, as described in detail in the Supplementary Materials. The likely order parameter in the SC_{FP} phase is therefore a two-component $B_{2u} + iB_{3u}$ which has \mathbf{m}_{orb} along the c -axis.

In summary, we present a three-dimensional mapping of SC_{FP} 's angular phase boundaries and unveil its true geometry. The physical picture that emerges is a magnetically-mediated superconducting state that appears only for fields tilted off UTe_2 's high-field magnetic easy axis (b) and can be made to persist beyond 73 T. Ginzburg-Landau modeling with a non-unitary spin triplet order parameter reproduces the distinct non-monotonic angle dependence of the upper critical field.

ACKNOWLEDGMENTS

We thank Daniel Agterberg for helpful discussions. This work was supported in part by the National Science Foundation under the Division of Materials Research Grant NSF-DMR 2105191. A portion of this work was performed at the National High Magnetic Field Laboratory (NHMFL), which is supported by National Science Foundation Cooperative Agreements DMR-1644779 and DMR-2128556, and the Department of Energy (DOE). Sample preparation and characterization was supported by the Department of Energy Award No. DE-SC-0019154 and the Gordon and Betty Moore Foundation's EPiQS Initiative through Grant No. GBMF9071. JS acknowledges support from the DOE BES program "Science of 100 T", which permitted the design and construction of much of the specialized equipment used in the high-field studies. The authors declare no competing financial interest. Identification of commercial equipment does not imply recommendation or endorsement by NIST.

-
- [1] S. Ran, C. Eckberg, Q.-P. Ding, Y. Furukawa, T. Metz, S. R. Saha, I.-L. Liu, M. Zic, H. Kim, J. Paglione, *et al.*, Nearly ferromagnetic spin-triplet superconductivity, *Science* **365**, 684 (2019).
 - [2] S. Ran, I.-L. Liu, Y. S. Eo, D. J. Campbell, P. M. Neves, W. T. Fuhrman, S. R. Saha, C. Eckberg, H. Kim, D. Graf, *et al.*, Extreme magnetic field-boosted superconductivity, *Nature physics* **15**, 1250 (2019).
 - [3] S. K. Lewin, C. E. Frank, S. Ran, J. Paglione, and N. P. Butch, A review of UTe_2 at high magnetic fields, *Reports on Progress in Physics* (2023).
 - [4] D. Aoki, J.-P. Brison, J. Flouquet, K. Ishida, G. Knebel, Y. Tokunaga, and Y. Yanase, Unconventional superconductivity in UTe_2 , *Journal of Physics: Condensed Matter* **34**, 243002 (2022).
 - [5] L. Jiao, S. Howard, S. Ran, Z. Wang, J. O. Rodriguez, M. Sigrist, Z. Wang, N. P. Butch, and V. Madhavan, Chiral superconductivity in heavy-fermion metal UTe_2 , *Nature* **579**, 523 (2020).
 - [6] I. Hayes, D. S. Wei, T. Metz, J. Zhang, Y. S. Eo, S. Ran, S. Saha, J. Collini, N. Butch, D. Agterberg, *et al.*, Multicomponent superconducting order parameter in UTe_2 , *Science* **373**, 797 (2021).
 - [7] G. Knebel, W. Knafo, A. Pourret, Q. Niu, M. Vališka,

- D. Braithwaite, G. Lapertot, M. Nardone, A. Zitouni, S. Mishra, *et al.*, Field-reentrant superconductivity close to a metamagnetic transition in the heavy-fermion superconductor UTe_2 , *Journal of the Physical Society of Japan* **88**, 063707 (2019).
- [8] H. Sakai, P. Opletal, Y. Tokiwa, E. Yamamoto, Y. Tokunaga, S. Kambe, and Y. Haga, Single crystal growth of superconducting UTe_2 by molten salt flux method, *Physical Review Materials* **6**, 073401 (2022).
- [9] Y. S. Eo, S. Liu, S. R. Saha, H. Kim, S. Ran, J. A. Horn, H. Hodovanets, J. Collini, T. Metz, W. T. Fuhrman, A. H. Nevidomskyy, J. D. Denlinger, N. P. Butch, M. S. Fuhrer, L. A. Wray, and J. Paglione, *c*-axis transport in UTe_2 : Evidence of three-dimensional conductivity component, *Phys. Rev. B* **106**, L060505 (2022).
- [10] T. Thebault, M. Vališka, G. Lapertot, A. Pourret, D. Aoki, G. Knebel, D. Braithwaite, and W. Knafo, Anisotropic signatures of electronic correlations in the electrical resistivity of UTe_2 , *Phys. Rev. B* **106**, 144406 (2022).
- [11] J. Lu, O. Zheliuk, I. Leermakers, N. F. Yuan, U. Zeitler, K. T. Law, and J. Ye, Evidence for two-dimensional in-plane superconductivity in gated MoS_2 , *Science* **350**, 1353 (2015).
- [12] J. Singleton and C. Mielke, Quasi-two-dimensional organic superconductors: A review, *arXiv preprint cond-mat/0202442* (2002).
- [13] L. Balicas, J. S. Brooks, K. Storr, S. Uji, M. Tokumoto, H. Tanaka, H. Kobayashi, A. Kobayashi, V. Barzykin, and L. P. Gor'kov, Superconductivity in an organic insulator at very high magnetic fields, *Phys. Rev. Lett.* **87**, 067002 (2001).
- [14] D. Aoki, K. Ishida, and J. Flouquet, Review of U-based ferromagnetic superconductors: comparison between UGe_2 , $URhGe$, and $UCoGe$, *Journal of the Physical Society of Japan* **88**, 022001 (2019).
- [15] F. Lévy, I. Sheikin, B. Grenier, and A. D. Huxley, Magnetic field-induced superconductivity in the ferromagnet $URhGe$, *Science* **309**, 1343 (2005).
- [16] W. Knafo, M. Nardone, M. Vališka, A. Zitouni, G. Lapertot, D. Aoki, G. Knebel, and D. Braithwaite, Comparison of two superconducting phases induced by a magnetic field in UTe_2 , *Communications Physics* **4**, 40 (2021).
- [17] W. Knafo, M. Vališka, D. Braithwaite, G. Lapertot, G. Knebel, A. Pourret, J.-P. Brison, J. Flouquet, and D. Aoki, Magnetic-field-induced phenomena in the paramagnetic superconductor UTe_2 , *Journal of the Physical Society of Japan* **88**, 063705 (2019).
- [18] M. Altarawneh, C. Mielke, and J. Brooks, Proximity detector circuits: An alternative to tunnel diode oscillators for contactless measurements in pulsed magnetic field environments, *Review of Scientific Instruments* **80** (2009).
- [19] S. Ran, S. R. Saha, I.-L. Liu, D. Graf, J. Paglione, and N. P. Butch, Expansion of the high field-boosted superconductivity in UTe_2 under pressure, *npj Quantum Materials* **6**, 75 (2021).
- [20] C. Broyles, Z. Rehfuss, H. Siddiquee, J. A. Zhu, K. Zheng, M. Nikolo, D. Graf, J. Singleton, and S. Ran, Revealing a 3d fermi surface pocket and electron-hole tunneling in UTe_2 with quantum oscillations, *Physical Review Letters* **131**, 036501 (2023).
- [21] Z. Wu, T. Weinberger, J. Chen, A. Cabala, D. Chichinadze, D. Shaffer, J. Pospisil, J. Prokleska, T. Haidamak, G. Bastien, *et al.*, Enhanced triplet superconductivity in next generation ultraclean UTe_2 , *arXiv preprint arXiv:2305.19033* (2023).
- [22] S. E. Sebastian, N. Harrison, and G. G. Lonzarich, Towards resolution of the fermi surface in underdoped high- T_c superconductors, *Reports on Progress in Physics* **75**, 102501 (2012).
- [23] M. Nikolo, J. Singleton, D. Solenov, J. Jiang, J. D. Weiss, and E. E. Hellstrom, Upper critical and irreversibility fields in $Ba(Fe_{0.92}Co_{0.08})_2As_2$ and $Ba(Fe_{0.91}Co_{0.09})_2As_2$ pnictide bulk superconductors, *Journal of Superconductivity and Novel Magnetism* **30**, 561 (2017).
- [24] M. Smylie, A. Koshchelev, K. Willa, R. Willa, W.-K. Kwok, J.-K. Bao, D. Chung, M. Kanatzidis, J. Singleton, F. Balakirev, *et al.*, Anisotropic upper critical field of pristine and proton-irradiated single crystals of the magnetically ordered superconductor $RbEuFe_4As_4$, *Physical Review B* **100**, 054507 (2019).
- [25] C. E. Frank, S. K. Lewin, G. S. Salas, P. Czajka, I. Hayes, H. Yoon, T. Metz, J. Paglione, J. Singleton, and N. P. Butch, Orphan high field superconductivity in non-superconducting Uranium Ditelluride, *arXiv preprint arXiv:2304.12392* (2023).
- [26] A. Miyake, Y. Shimizu, Y. J. Sato, D. Li, A. Nakamura, Y. Homma, F. Honda, J. Flouquet, M. Tokunaga, and D. Aoki, Metamagnetic transition in heavy fermion superconductor UTe_2 , *Journal of the Physical Society of Japan* **88**, 063706 (2019).

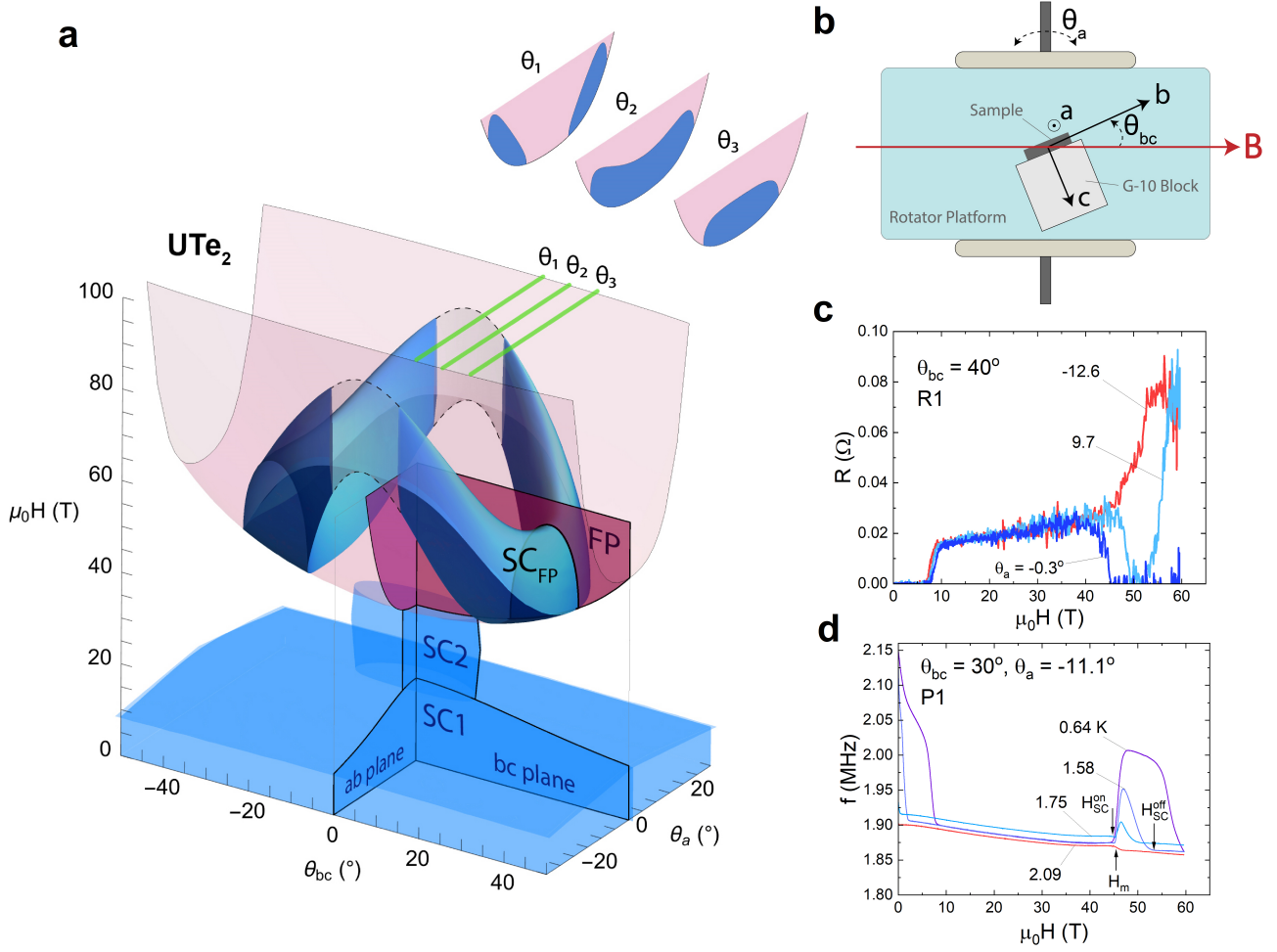


FIG. 1. Field-angle phase diagram of UTe_2 and experimental details. (a) Illustration of UTe_2 's field-dependent phase diagram, with the ab and bc planes highlighted. The three superconducting regions are shown in blue. The boundaries of the low-field SC1 phase vary smoothly with the field direction, while the field-stabilized SC2 phase exists only for fields near the b axis. The SC_{FP} state appears inside the field-polarized state (pink) only for specific off-axis fields that yield the saddle-like shape in the drawing. (b) Depiction of measurement setup that enables effective dual-axis rotation. The crystal (gray) is placed on a block (white) on the rotator platform at a fixed angle within the bc plane (θ_{bc}); the angle off the bc plane (θ_a) is set to different values during the experiment. (c) Electrical resistance R vs. field at various θ_a for sample R1, which reveal the high-field zero-resistance SC_{FP} state. (d) PDO data obtained at various temperatures for sample P1. An abrupt jump in f (indicating a transition to a low resistance state) is no longer observed at 2.09 K, consistent with a loss of superconductivity at that temperature.

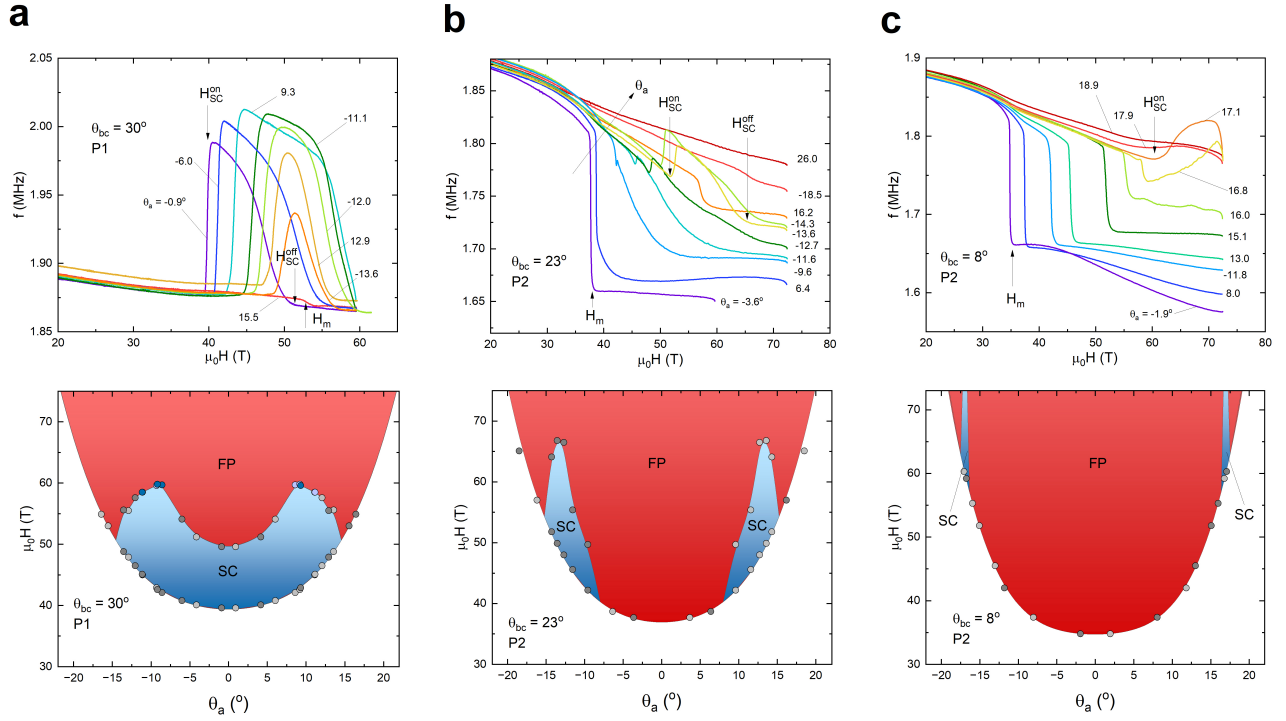


FIG. 2. **Angle-dependent PDO data and corresponding phase diagrams.** PDO data (frequency vs. magnetic field) and corresponding phase diagrams collected at (a) $\theta_{bc} = 30^\circ$, (b) 23° , and (c) 8° . An abrupt increase in f indicates a superconducting transition while a drop indicates a metamagnetic transition into the field-polarized phase. Superconducting regions are colored blue while the electrically resistive portions of the field polarized state are colored red. The phase diagrams have been symmetrized for clarity. This is justified by the underlying crystal symmetry and the absence of any observed symmetry breaking in our measurements. Darker points indicate θ_a values at which pulses were performed while light points have been added at the corresponding $-\theta_a$ for clarity. The blue points in the phase diagram of (a) indicate that the phase transition itself was above the measured field range and was identified via extrapolation, as described in the Supplementary Materials.

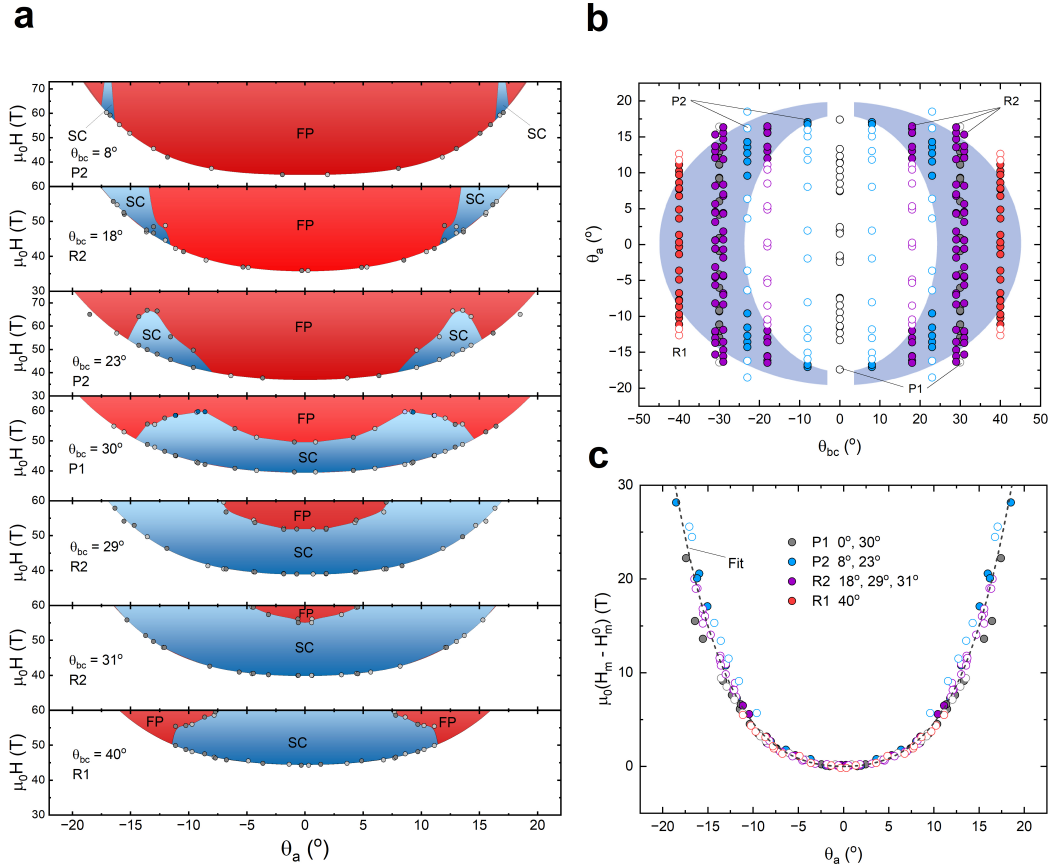


FIG. 3. **Halo geometry of SC_{FP} state.** (a) High-field phase diagrams presented as a function of θ_a collected at fixed θ_{bc} . Red indicates resistive regions of the FP phase while blue indicates superconducting regions. The gray points represent the measured phase boundaries from which the plots are constructed, with the dark (light) points corresponding to actual (symmetrized) data. (b) Pure angular (θ_{bc} vs. θ_a) representation of the superconducting phase boundaries. Full circles are used for angles at which superconductivity is observed while open circles indicate that only a metamagnetic transition is seen. Different colors indicate different samples. Data are symmetrized to populate all four quadrants for clarity. The blue halo is for illustrative purposes, to emphasize that superconductivity is caused by tilting \mathbf{H} off b . (c) Measured transition field minus $H_m^0(\theta_{bc})$, plotted as a function of θ_a . As above, full circles indicate a superconducting transition while open circles indicate that only a metamagnetic transition is seen. For a given θ_{bc} , $H_m^0(\theta_{bc})$ is the metamagnetic transition field at $\theta_a = 0$. The legend indicates which colors are used for which sample and the θ_{bc} values at which data was collected. The dotted line is a fit of the entire data set to Eq. 1 after subtracting off the individual $H_m^0(\theta_{bc})$ values.